Linking geomechanical simulation of induced seismicity to surface seismic observations Simulated finite fault rupture to moment tensor inversion

Ruan, Jingming; Masfara, La Ode Marzujriban; Ghose, Ranajit; Mulder, Wim

DOI
10.1190/image2022-3751471.1

Publication date
2022

Document Version
Final published version

Published in
Second International Meeting for Applied Geoscience and Energy

Linking geomechanical simulation of induced seismicity to surface seismic observations: simulated finite fault rupture to moment tensor inversion

Jingming Ruan, La Ode Marzujriban Masfara, Ranajit Ghose, Delft University of Technology; Wim Mulder, Shell Global Solutions International BV*

SUMMARY

Dynamic geomechanical modeling can generate the seismic wavefield caused by a fault rupture. In dynamic fault-rupture modeling, the source is considered to be finite, with a limited extent both in space and in time. This contrasts with the definition of a point source, which is generally assumed to explain the seismic wavefield caused by an earthquake. Most earlier seismic inversion studies, including those of the induced earthquakes caused by depletion of the Groningen gas field, were performed assuming a point source. Still, finding a point-source reference from the seismic wavefield, even when generated by finite faulting, is important in order to calibrate the geomechanical simulation with field-seismic observations. To this end, we have developed a workflow that links geomechanical forward modeling to seismic moment tensor inversion. We have tested this workflow for the dynamic rupture considering a realistic 3D layered earth model. At first, we simulate the triggering of dynamic fault slip at the center of a fault plane. Next, we invert the seismograms recorded by receivers located on or near the surface to obtain the full moment-tensor point-source representation and the location of the earthquake. The results of inversion show similar waveforms for both the point source and the finite source. The location of the inverted point source is within 400 m from the center of the slip patch. The double-couple components of the inverted moment tensor also match with the strike and the dip of the fault plane.

INTRODUCTION

Induced earthquakes are caused by human activities. These events are under intensive investigation in many regions on Earth, such as the Groningen gas field–the largest gas field in Europe and the tenth largest in the world. Numerous studies have been carried out for the Groningen gas field addressing underground structures, material properties, and reservoir history due to gas production, which is the main cause for the induced earthquakes in the region. Geomechanical modeling is widely used to simulate the physical processes associated with induced earthquakes, based on the available background information. The simulation normally consists of two parts. In the first part, the stress field variation inside the reservoir and the surrounding formations due to gas production is simulated. The second part involves a dynamic simulation, after the fault becomes critical when the shear stress exceeds the fault strength. From the dynamic simulation, the dynamic rupture and the resulting seismic wavefield are modeled, the latter representing the wavefield generated by a finite source. This finite source is typically a displacement function of space and time on the fault and is different from the widely used point-source assumption made in seismic forward modeling, which represents a displacement function of time at a single location.

The commonly used constraints in geomechanical modeling of induced seismicity are the production history and the magnitude of prior earthquakes. Field seismic observations are mostly neglected when calibrating the dynamic rupture modeling. One of the primary reasons for this is the fact that most earlier attempts of seismic inversion studies, including those in Groningen, assumed a point source, thus not allowing for a direct link with the rupture of a finite fault as used in geomechanical modeling.

To link geomechanical modeling to field-seismic observations, in this research we introduce a workflow to obtain a point-source representation using the wavefield generated from geomechanical modeling. We started with 3D geomechanical modeling of a fault rupture and simulating the resulting (synthetic) seismic wavefield. We then performed a probabilistic inversion of the synthetic seismic data observed near the surface. In the end, our workflow provided a point-source with its full moment tensor representation and the centroid locations. The point-source representation can serve as a reference to evaluate the point source inverted from the field-seismic data. With this workflow, the field seismic observations can be used as constraints for geomechanical modeling, when simulating the dynamic rupture.

GEOMECHANICAL SIMULATION

Many earlier studies based on laboratory experiments and numerical modeling have shown that the stress change due to gas production is the main cause of the induced earthquakes in the Groningen region. Stress changes in a depleting reservoir is normally considered as a poroelastic process; thus modeling the long-term gas production effects requires solving the poroelastic equations. Nevertheless, the duration of a seismic event is much shorter (<10 s) compared to the long time span of gas extraction, which is normally in the order of days, weeks, or even months. Therefore, it is reasonable to consider little to no pressure variation throughout the process of the dynamic rupture. In this study, we have investigated a model with critical initial stresses in order to simulate the stress field after sufficient gas production. We start with a dynamic rupture simulating the process of fault slip, followed by a simulation of the seismic wave propagation. At this stage, we need to solve the elastodynamic problem described by the governing system of equations for the displacement vector $\mathbf{u}$:

$$\mathbf{M}\ddot{\mathbf{u}} + \mathbf{C}\dot{\mathbf{u}} + \mathbf{K}\mathbf{u} = \mathbf{f}, \tag{1}$$

where $\mathbf{M}$ is the mass matrix, $\mathbf{C} = \alpha_\eta \mathbf{M} + \beta_\eta \mathbf{K}$ is the damping matrix with α and β the Rayleigh damping coefficients, $\mathbf{K}$ the stiffness matrix, and $\mathbf{f}$ the source term. The system is solved

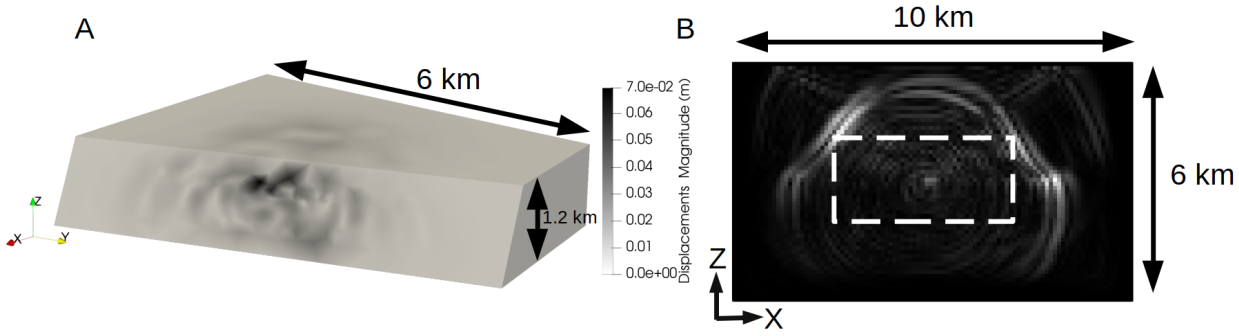

Figure 1: Snapshots of dynamic rupture and the simulated seismic wavefield. A: snapshot of dynamic rupture obtained from the geomechanical simulation, showing the displacement field on the footwall of the model. The model contains a slanted fault, which is shown in the front face in the figure. B: snapshot of the velocity field obtained from the wavefield simulation. The white dashed rectangle marks the sub-domain of the geomechanical model, which is enclosed by the finite-difference wave-propagation model.

with the incremental form of the Newmark explicit scheme, which can be written as follows:

$$\begin{aligned}\Delta\mathbf{u}_n =& \mathbf{M}^{-1}\left(\Delta t^2\left(\Delta\mathbf{f}_n - \mathbf{K}\Delta\mathbf{u}_{n-1}\right) - \Delta t\,\mathbf{C}\left(\Delta\mathbf{u}_{n-1} - \Delta\mathbf{u}_{n-2}\right)\right)\\ &+ 2\Delta\mathbf{u}_{n-1} - \Delta\mathbf{u}_{n-2},\end{aligned} \tag{2}$$

where n refers to time t_n. Equation (2) gives the unconstrained dynamic solution for the whole medium except for the constrained fault moment. In our study, the implementation of the fault in 3D geomechanical modeling is realized by splitting the fault nodes to elements located on both sides of the fault. Depending on whether the fault is locked or slipping, the displacement of the separated node pairs is constrained differently in tangent and normal directions. The slipping movement on the fault is given by the forward incremental Lagrange Multiplier method (see Meng (2017)):

$$\begin{aligned}\lambda_n &= \left(\Delta t^2\mathbf{G}\mathbf{M}^{-1}\mathbf{G}^T\right)^{-1}\left(\mathbf{G}\Delta\mathbf{u}_n - \mathbf{I}_n\right)\Delta\mathbf{u}_n\\ &= \Delta\mathbf{u}_n - \Delta t^2\mathbf{M}^{-1}\mathbf{G}^T\lambda_n,\end{aligned} \tag{3}$$

where the Lagrange Multiplier λ_n is the nodal force needed to constrain the solution $\mathbf{u}_n$, making λ_n a proxy for the stress on the fault.

For the geomechanical simulations, we used the finite element (FE) code Defmod by Ali (2014) and Meng (2017). For the wavefield simulation, we used the finite difference (FD) code OpenSWPC by Maeda et al. (2017). The coupling between Defmod and OpenSWPC was developed by Meng and Wang (2018). Due to the relatively intensive computation involved in the finite element simulation, we chose to limit the domain of geomechanical modeling to the depth interval of the reservoir and some parts of the surrounding formations. The geomechanical modeling provides the displacement on the fault, which can then be injected into the finite difference code as a number of point sources to simulate the seismic wave propagation. The source-time functions of the point sources were imposed based on the displacement field on the fault plane in order to generate a finite source.

PROBABILISTIC INVERSION

After the simulation of the dynamic rupture and the resulting (synthetic) seismic wavefield, we use the synthetic surface-seismic data in a probabilistic inversion developed by Masfara et al. (2021) to obtain a point-source representation. The probabilistic inversion workflow involves a linearized variant of the Hamiltonian Monte Carlo (HMC) algorithm, which is highly efficient in sampling higher-dimensional model spaces. The inversion strongly depends on the quality of the prior, which includes the moment tensor, centroid, and the origin time of the earthquake. Because the prior information can be retrieved from the dynamic rupture simulation, this method is suitable for inverting the point source from the wavefield synthesized from the dynamic rupture. We used the location and the origin time of the rupture as prior information in the inversion. Due to the inhomogeneous nature of the medium and the anisotropic rupture movement, the a-priori information of the moment tensor is not available for inversion when using a finite source. Because the rupture always starts from the beginning of the dynamic simulation, the origin time is always set to 0 s (prior information).

Before performing the probabilistic inversion, we need to solve the forward problem, which results in surface displacements due to an earthquake, given a description of the earthquake in terms of elementary moment tensors. The seismograms derived from solving the forward problem depend on the medium. Therefore, we solved the forward problem using the same model setup as in the geomechanical model. We then applied the workflow to invert for the moment tensor and the location of the representative point-source, using the wavefield generated by the *finite* source. As the slip patch was determined by an assumed initial stress field, we could also choose to invert for the moment tensor only, while keeping the source location fixed.

EXAMPLE

We present an example using the new workflow involving probabilistic inversion of the wavefield generated from a dynamic

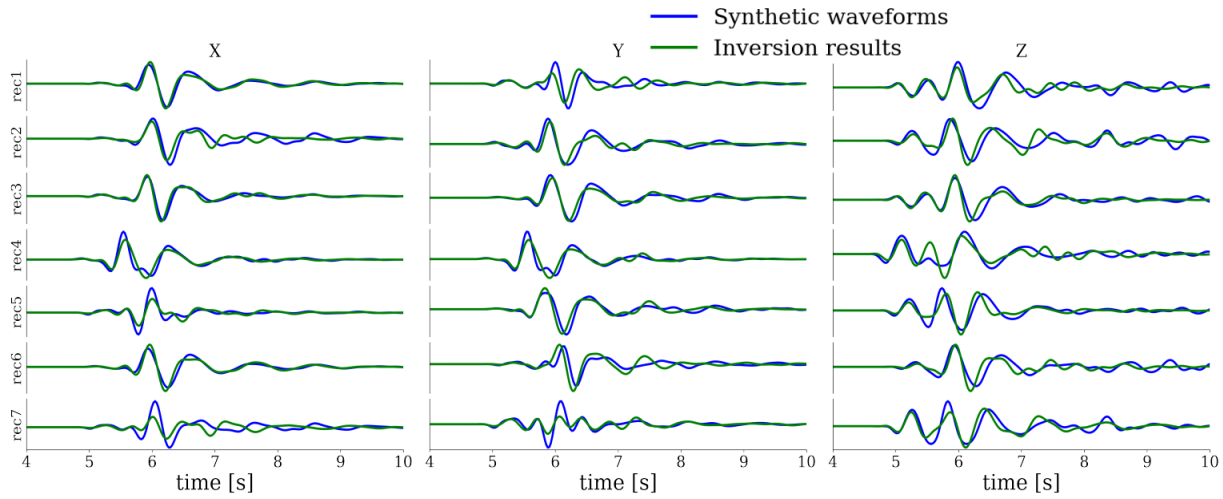

Figure 2: Comparison of synthetic seismograms from geomechanical modeling (finite source) with seismograms obtained from an inverted point source, at seven receivers located 200 m below the surface of the model. The seismograms represent the X, Y, and Z components of the displacement. Synthetic waveforms represent seismograms generated from the simulated dynamic rupture (geomechanical modeling); inversion results are the seismograms generated using the point source inverted from the seismic data generated by the dynamic rupture.

rupture, i.e., geomechanical simulation of a finite-fault slip. The model used is a layered-earth model with a slanted fault cutting through the entire domain, as shown in Figure 1. The layered medium is homogeneous in the lateral directions and is divided into three layers in the depth direction, to simulate the simplified underground structure of the Groningen gas field, representing the overburden, the reservoir, and the basement.

We assume an initial stress field with a critically stressed slip patch of 100 m $\times$ 100 m, where the shear stress is larger than the fault strength. The slip patch is located in the center of the fault and inside the reservoir interval, while the rest of the fault remains stable during the simulation.

After the initial loading, we simulate the dynamic rupture. We then inject the finite-fault-slip data into the finite difference wavefield modeling to obtain the surface-seismic observations. Meanwhile, we calculate the elementary seismograms for the same medium, which are subsequently used as a database for the probabilistic inversion. The finite element model for geomechanical modeling has a small element size close to the fault, whereas the element size increases away from it. In this case, the characteristic length of an element is 100 m near the fault and 400 m far away from the fault. We used a finite difference mesh with a 100-m spacing for the wavefield simulation.

We apply a band-pass filter (1-3 Hz) to both the seismic data at the seven receiver stations in the model and to the elementary seismograms. We then apply probabilistic inversion to the filtered receiver data. Through using the inverted moment tensor and the elementary seismograms, we compute the receiver data generated by the inverted point source, which is subsequently compared with the seismograms obtained from geomechanical modeling. In additional, we compare the inverted moment tensor with the average strike, dip and rake of the simulated rupture.

The point-source representation shows a good fit to the seismograms in the 1-3 Hz frequency band, as can be seen in Figure 2. The location of the inverted point source also shows a good match in the X coordinate, while both the Y and Z coordinates are within 300 m from the center of the slip patch. We calculate the beach-ball model of source moment tensor from the dynamic rupture based on its average strike, dip and rake. The comparison of this moment tensor with the inverted point-source moment tensor is shown in Figure 3, illustrating the full moment tensor and only the double-couple (DC) components of the moment tensor. The comparison is limited to the DC component, because the strike, dip and rake provide only the DC components of the moment tensor.

The comparison shows a good similarity in both strike and dip. However, the rake direction is different: the dynamic rupture shows a major normal faulting, while the point-source representation indicates a strike-slip event. The cause of the misfit may be related to our assumption of a laterally homogeneous subsurface, which caused a smooth distribution of the first-arrival time, making it difficult for the inversion to minimize the misfit for both source location and the first-arrival time. If a model with a realistic lateral heterogeneity is used, the inversion should give a more accurate point-source location.

CONCLUSION

We have presented a workflow for obtaining a point-source representation from the wavefield generated by the dynamic rupture of a finite fault by 3D poroelastic modeling for a model of the Groningen gas reservoir. The workflow starts with geomechanical modeling, which simulates the dynamic rupture

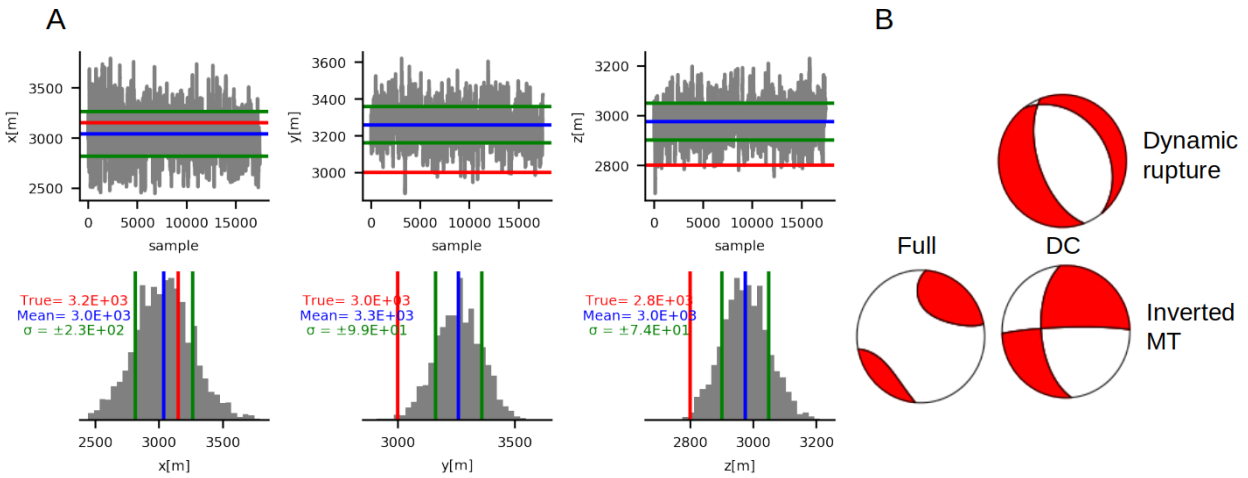

Figure 3: A: The posterior distribution of the point source location. The "True" values indicate the location of the center of the slip patch. B: Beach-ball models of the source moment tensor from the dynamic rupture and the inverted point source. The beach-ball model from the dynamic rupture is transformed using the average strike, dip and rake of the fault. The inverted moment tensor is depicted, with both the full moment tensor and with only the double-couple components.

due to a given stress field evolution. With the simulated rupture, we estimate the surface seismic displacements through finite-difference modeling of the wave propagation. By using a probabilistic inversion of the seismograms representing (near)surface-observation, we obtain a point-source representation from the finite-fault rupture.

In this example, we have tested the workflow using a layered-earth model containing a slanted fault. Our results show that the inverted point source has a seismic response which is similar to the response from the geomechanically simulated finite faulting, at all seven receiver locations. By comparing the DC component of the inverted moment tensor with that calculated from the average movement of the modeled finite fault, we found that the inverted point source shows a strike and dip similar to those corresponding to the finite-fault rupture. The location of the point source is, however, less accurate, but still within 400 m from the center of the rupture patch. The rake direction given by the DC components of the inverted moment tensor indicates a strike-slip event, while the dynamic rupture shows a prominent normal faulting.

The presented workflow provides a point-source representation obtained from the dynamic rupture of a finite fault that is similar to the wavefield observed in the Groningen gas field. The workflow enables a connection between the geomechanical modeling of a finite fault and the field-seismic observation, which contrasts with the point-source assumption usually made when inverting field-seismic observations. If a more realistic, heterogeneous underground structure is used, we anticipate that the accuracy of the inversion will be improved, compared with the layered-earth model with lateral homogeneity that has so far been assumed in our study. In future work, we will apply the workflow on a more realistic model of the Groningen subsurface and seismic data from induced earthquakes, recorded in wells.

ACKNOWLEDGMENTS

We thank Takuto Maeda for making OpenSWPC open-source. We are grateful to Chunfang Meng for providing the geomechanical simulation code with the hybrid solver and coupling FE-FD code Defmod-SWPC, as well as guidance on model design.

REFERENCES

Ali, S. T., 2014, Defmod-parallel multiphysics finite element code for modeling crustal deformation during the earthquake/rifting cycle: arXiv:1402.0429.

Maeda, T., S. Takemura, and T. Furumura, 2017, Openswpc: an open-source integrated parallel simulation code for modeling seismic wave propagation in 3d heterogeneous viscoelastic media: Earth, Planets and Space, **69**, 1–20, doi: https://doi.org/10.1186/s40623-017-0687-2.

Masfara, L. O. M., C. Weemstra, and T. Cullison, 2021, Efficient probabilistic inversion of induced earthquake parameters in 3d heterogeneous media: Solid Earth Discussions, 1–5, doi: https://doi.org/10.5194/se-2021-156.

Meng, C., 2017, Benchmarking Defmod, an open source FEM code for modeling episodic fault rupture: Computers & Geosciences, **100**, 10–26, doi: https://doi.org/10.1016/j.cageo.2016.11.014.

Meng, C., and H. Wang, 2018, A finite element and finite difference mixed approach for modeling fault rupture and ground motion: Computers & Geosciences, **113**, 54–69, doi: https://doi.org/10.1016/j.cageo.2018.01.015.